

UC Irvine

UC Irvine Previously Published Works

Title

Scaling gross ecosystem production at Harvard Forest with remote sensing: a comparison of estimates from a constrained quantum-use efficiency model and eddy correlation

Permalink

<https://escholarship.org/uc/item/7ht7565c>

Journal

Plant Cell & Environment, 18(10)

ISSN

0140-7791

Authors

WARING, RH
LAW, BE
GOULDEN, ML
[et al.](#)

Publication Date

1995-10-01

DOI

10.1111/j.1365-3040.1995.tb00629.x

Copyright Information

This work is made available under the terms of a Creative Commons Attribution License, available at <https://creativecommons.org/licenses/by/4.0/>

Peer reviewed

Scaling gross ecosystem production at Harvard Forest with remote sensing: a comparison of estimates from a constrained quantum-use efficiency model and eddy correlation

R.H. WARING,¹ B.E. LAW,¹ M.L. GOULDEN,² S.L. BASSOW,³ R.W. McCREIGHT,¹ S.C. WOFSY² & F.A. BAZZAZ³

¹College of Forestry, Oregon State University, Corvallis, OR 97331, ²Division of Applied Sciences and Department of Earth and Planetary Science, Harvard University, Cambridge, MA 02138, and ³Department of Organismic and Evolutionary Biology, Harvard University, Cambridge, MA 02138 USA

ABSTRACT

Two independent methods of estimating gross ecosystem production (GEP) were compared over a period of 2 years at monthly integrals for a mixed forest of conifers and deciduous hardwoods at Harvard Forest in central Massachusetts. Continuous eddy flux measurements of net ecosystem exchange (NEE) provided one estimate of GEP by taking day to night temperature differences into account to estimate autotrophic and heterotrophic respiration. GEP was also estimated with a quantum efficiency model based on measurements of maximum quantum efficiency (Q_{\max}), seasonal variation in canopy phenology and chlorophyll content, incident PAR, and the constraints of freezing temperatures and vapour pressure deficits on stomatal conductance. Quantum efficiency model estimates of GEP and those derived from eddy flux measurements compared well at monthly integrals over two consecutive years ($R^2 = 0.98$).

Remotely sensed data were acquired seasonally with an ultralight aircraft to provide a means of scaling the leaf area and leaf pigmentation changes that affected the light absorption of photosynthetically active radiation to larger areas. A linear correlation between chlorophyll concentrations in the upper canopy leaves of four hardwood species and their quantum efficiencies ($R^2 = 0.99$) suggested that seasonal changes in quantum efficiency for the entire canopy can be quantified with remotely sensed indices of chlorophyll. Analysis of video data collected from the ultralight aircraft indicated that the fraction of conifer cover varied from < 7% near the instrument tower to about 25% for a larger sized area. At 25% conifer cover, the quantum efficiency model predicted an increase in the estimate of annual GEP of < 5% because unfavourable environmental conditions limited conifer photosynthesis in much of the non-growing season when hardwoods lacked leaves.

Key-words: canopy chlorophyll content; canopy photosynthesis; CO₂ eddy flux; modelling; NDVI; quantum-use efficiency; remote sensing.

INTRODUCTION

In most ecosystem models the general assumption is made that photosynthesis by an entire canopy is usually light-limited and, as a result, that the assimilation rate can be assumed to be near linearly related to the absorbed flux density of photosynthetically active radiation (Jarvis & Leverenz 1983). This assumption has been widely accepted, variation in the efficiency by which PAR is absorbed under diffuse and direct-beam solar radiation at varying solar zenith angles being taken into account (Charles-Edwards 1982; Wang, McMurtrie & Landsberg 1992). If solar radiation data over periods of months or longer are integrated, the linearity of canopy photosynthetic response to absorbed photosynthetically active radiation increases as differences in the beam fraction and solar zenith angle of incident PAR are balanced out (Wang & Polglase 1995). To date, support for a simple canopy light-absorption model has been provided mainly from studies on homogeneous canopies of single-species composition (Baker, Hesketh & Duncan 1972; McCree 1984; Caldwell *et al.* 1986).

Natural vegetation is often a mixture of species or varies in structure, in contrast to a homogeneous monoculture of crops or tree plantations. It is desirable therefore to test how well the linear light absorption model applies to vegetation composed of a mixture of species. We had such an opportunity at the Harvard Forest which is situated in the temperate forest region of the northeastern USA. There, long-term studies of physiology and ecology have been combined with continuous eddy flux data since 1990 which provide measures of whole-system net ecosystem exchange (NEE) and gross ecosystem production (GEP) (Wofsy *et al.* 1993).

Calculations of net ecosystem production showed that Harvard Forest was accumulating 2–4 Mg C ha⁻¹ annually in biomass and soil organic matter (Wofsy *et al.* 1993), an

interpretation that may apply to a wide range of temperate forests (Tans, Fung & Takahashi 1990). To date, few ecosystem models have been scaled regionally to evaluate these predictions. Most models are not dynamic, in the sense that vegetation boundaries, phenology, and weather conditions are assumed to be stable from year to year (Melillo *et al.* 1993; Potter *et al.* 1994).

To make regional or global scale models more dynamic, there has been an effort to integrate satellite-derived data in a form useful for parametrizing and driving simplified ecosystem models. Current global satellite coverage can provide remotely sensed estimates of solar radiation, ambient air temperature, atmospheric humidity deficits and surface moisture conditions for areas of the order of 25–100 km² or larger (Dye & Goward 1993; Waring *et al.* 1993; Goward *et al.* 1994a; Prince & Goward 1995). In addition, spectral vegetation indices, calculated from the red (R) and near-infrared (NIR) portions of the spectrum, provide indicators of seasonal changes in the amount of green leaf cover (Kumar & Monteith 1982). Studies have shown that the normalized difference vegetation index [NDVI: (NIR-R)/(NIR + R)] is a linear to near-linear function of the fraction of photosynthetically active radiation (PAR) intercepted by many types of green vegetation (Asrar *et al.* 1984; Law & Waring 1994a,b; Goward *et al.* 1994a). Monthly integration of data is usually required to reduce errors to less than 5% in estimating solar radiation and to obtain cloud-free estimates of canopy properties and surface moisture conditions by remote sensing (Goward *et al.* 1994a). In combination, these remotely sensed variables are employed to provide time-integrated estimates of photosynthesis across landscapes for broadly similar types of vegetation, given knowledge of the apparent quantum efficiency of canopies and the extent to which environmental factors constrain stomatal conductance (Running *et al.* 1989; Sellers *et al.* 1992; Nemani, Pierce & Running 1993; Verma *et al.* 1993).

At Harvard Forest, all the requisite data required to drive the photosynthetic component of a whole-system model were available. A tower equipped with eddy-flux instrumentation provided an estimate of gross ecosystem production (GEP) that could be compared to independent estimates of GEP derived from a model based on measurements of maximum quantum efficiency (Q_{max}), seasonal variation in canopy leaf area index, leaf chlorophyll content, incident PAR, and restriction on CO₂ diffusion through stomata imposed by freezing temperatures, vapour pressure deficits and other environmental factors.

From an Oregon State University ultralight aircraft, video and spectroradiometer data were acquired seasonally to provide the necessary spatial resolution to characterize variation in conifer and deciduous hardwood cover and to document pigment and leaf area changes in the hardwood component of the canopy. With remotely sensed data obtained from the aircraft we gained an independent measure of phenology to compare with that obtained from ground observations. In this paper we compare predictions of monthly gross ecosystem production derived from the

quantum efficiency model with those determined by eddy correlation and suggest how remotely sensed data can aid in scaling stand-level observations to larger areas.

METHODS

Site description

The study site was located in the Prospect Hill tract of Harvard Forest, north-central Massachusetts (42.54° N 72.18° W; elevation 340 m). The forest, composed of 50- to 70-year-old trees, regenerated following a hurricane in 1938 and has reached a height of 20–24 m and supports a leaf area index of between 3.5 and 4.0 during the growing season. At present, dominant species are red oak (*Quercus rubra* L.) and red maple (*Acer rubrum* L.), which together make up 80% of the total 30 m² ha⁻¹ of basal area. Some black birch (*Betula lenta* L.), white birch (*Betula papyrifera* Marsh.), yellow birch (*Betula alleghaniensis* Britton), black cherry (*Prunus serotina* Ehrh.), white pine (*Pinus strobus* L.), and hemlock (*Tsuga canadensis* (L.) Carr.) are also present, but together represent less than 20% of the total basal area and less than 10% of the 1300 stems ha⁻¹. The climate is cool temperate (January mean weekly temperature -6 °C, July mean 20 °C), and humid, with precipitation distributed evenly throughout the year (annual mean 1100 mm). Summer drought rarely occurs. The terrain is moderately hilly, about 95% forested, with the nearest paved roads > 1 km away and small towns >10 km away. Soils are mainly of the Gloucester series (fine loamy, mixed mesic Typic Dystrochrept) with a surface pH of 3.8 and a subsurface pH of 4.8 (Peterjohn *et al.* 1994).

Meteorological data

Meteorological sensors were installed at the top of a 30 m tower (Rohn 25G), 6–10 m above the top of the forest canopy (Wofsy *et al.* 1993). Data were logged on a computer situated in a climate-controlled shack 20 m from the base of the tower. Throughout the investigation, the system logged 60 min mean air temperature measured with an aspirated thermistor, relative humidity determined with an electrical-capacitance sensor, and horizontal photosynthetically active photon flux density obtained with a pair of silicon quantum sensors one above the canopy and the other below at a height of 8 m. The soil-surface temperature was also recorded using an array of potted thermistors. An integrated monthly measure of the fraction of light intercepted by the canopy (f_{IPAR}) was subsequently calculated as 1 – the fraction of incident PAR that was transmitted through the canopy.

The observations were interrupted by occasional extended gaps as a result of equipment failure, and by more frequent gaps associated with calibration, maintenance or data transfer. The meteorological data for 1991 were comparatively patchy, with 20% missing, while 10% were missing for 1992. In the current analysis we replaced miss-

ing meteorological data with the mean for that hour plus and minus 2 d.

Eddy flux measurements

Eddy-correlation measurements of net ecosystem CO₂ exchange were initiated at Harvard Forest in April 1990 on the same 30 m tower where meteorological instruments were installed. A three-axis sonic anemometer (Applied Technologies) and a closed-path infrared gas analyser (IRGA, LiCor 6262 or 6251) were used to sample simultaneously the vertical wind speed and the CO₂ mixing concentration at 30 m. The raw signals were digitized at 4 Hz and these data logged to disk for subsequent analysis. Air was drawn to the instrument shelter down a 50 m tube and through the IRGA at 6 to 8 dm³ min⁻¹, introducing a lag of several seconds which we adjusted for in the flux calculation (Wofsy *et al.* 1993; Fan *et al.* 1995). In computing the flux we accounted for the orientation of the streamlines by rotation to the plane where the mean vertical wind speed was zero (McMillen 1988).

A series of simulations, laboratory tests, and spectral analyses indicated a small underestimation of flux caused by the reliance on a closed path sensor for the CO₂ measurement (overall 90% response faster than 1 s). We corrected for this error by scaling the measured CO₂ flux by the ratio of the measured raw sensible heat flux to the sensible heat flux calculated after filtering the temperature signal to simulate an instrument with limited high-frequency response (Leuning & King 1992; Wofsy *et al.* 1993). This correction was generally small (<10%) because most flux is carried by eddies with a frequency of 0.1 to 0.002 Hz. Uncertainty associated with calibration was less than 10%. Additionally, we anticipate <10% underestimation of flux caused by finite sensor path length and spatial separation (Baldocchi & Meyers 1991; Lee & Black 1994). Data gaps occurred occasionally, particularly following lightning strikes. For these gaps we substituted values from hourly averages determined from the closest 5 d set of data.

Changes in atmospheric stability may cause shifts in the quantity of CO₂ stored in the air space below the sensor array, decoupling the flux through the eddy plane from biotic activity. We accounted for storage by monitoring the change in CO₂ in the air space beneath 30 m with a second IRGA to sample sequentially inlets at 29, 24, 18, 12, 5, 3, 1 and 0.5 m. We then applied the rate of CO₂ storage change in combination with the eddy flux measurement to calculate net ecosystem exchange (NEE) (Wofsy *et al.* 1993).

In the convention of eddy-flux measurements, photosynthesis is a negative flux into the system and respiration is a positive flux out. Net ecosystem exchange measured during daylight hours includes gross photosynthesis (P_g) photorespiration (R_p), maintenance respiration (R_m) and growth respiration (R_g) of autotrophic plants as well as all sources of heterotrophic respiration (R_h).

$$\text{Day NEE} = P_g + R_p + R_m + R_g + R_h \quad (1)$$

At night the photosynthetic terms, P_g and R_p , are absent.

$$\text{Night NEE} = R_m + R_g + R_h = R_e \quad (2)$$

where R_e is the total ecosystem respiration. R_m and R_h are largely controlled by temperature, allowing us to approximate R_e during daylight periods as a function of temperature. The relation between Night NEE during well mixed periods (Fan *et al.* 1995) and soil temperature (T_s) was

$$\text{Day } R_e \text{ (}\mu\text{mol m}^{-2} \text{ s}^{-1}\text{)} = T_s (0.19) + 0.795 \quad (3)$$

Gross ecosystem production (GEP) is then calculated as

$$\text{GEP} = \text{Day NEE} - \text{Day } R_e = P_g + R_p \quad (4)$$

Day R_e is typically 20–30% of Day NEE. Consequently, large uncertainties in Day R_e have a relatively small effect on the accuracy of GEP.

Vegetation measurements

The basal area of tree species was determined by measuring tree diameters at breast height (1.37 m) in a 50 m × 50 m plot centred 100 m south of the eddy flux tower. Within the same area, leaf litter was collected in 35 0.122 m² traps to estimate the leaf area index (LAI) of deciduous hardwoods and the relative contribution of each species. Fewer than 10 white pine tree stems were present within the sampling area and were excluded from the analysis. Independent estimates of maximum and minimum LAI, which did include the conifers, were made in the same area using a LiCor LAI 2000 Plant Canopy Analyzer (Welles & Norman 1991). Phenological observations were provided by John O'Keefe at Harvard Forest, who recorded the dates of initial bud break, when leaves were at 75 and 95% of full expansion, when autumn colour was first observed, and when 10–25 and 98% of leaves had been shed. These data were available for all major tree species but we referenced whole-canopy phenology to only the two dominant species, red oak and red maple.

Apparent maximum quantum efficiency was determined in August when leaves were fully expanded on four hardwood species from samples of representative leaves growing near the top of the canopy. A Li-Cor 6200 gas exchange system (Lincoln, NE, USA) equipped with a 0.25 dm³ cuvette and a PAR sensor was used to obtain measurements of dark respiration, net photosynthesis and photon flux density. Neutral shade cloth incrementally reduced the light level incident on the leaf surface, allowing for repeated measurements of the same leaves at different light levels. Leaves were allowed to acclimate to the light levels for at least 5 to 8 min before instantaneous gas exchange measurements were taken. For red oak and red maple, measurements were made on 10 leaves located in the upper canopy and an additional 10 in the lower canopy strata (five leaves at both heights on two trees of each species). For other species, measurements were made on five leaves from each strata (one tree per species). Apparent maximum quantum efficiency and maximum

photosynthetic rates were determined from least-squares fitting of the basic photosynthesis, light-saturation equation described by Ögren & Evans (1993):

$$CP^2 - (Q_{\max} + PAR + P_m)P - Q_{\max} + PAR + P_m = 0, \quad (5)$$

where P is the photosynthetic rate, PAR is the incident PAR irradiance, Q_{\max} is the apparent maximum quantum efficiency, P_m is the maximum photosynthetic rate at light saturation, and C is the curvature of the light saturation curve at ambient CO_2 and O_2 partial pressure observed in our field analysis. The apparent maximum quantum efficiency is determined from the linear portion of the CO_2 uptake response as incident PAR increases from zero. Gross photosynthesis (P_g), leaf maintenance respiration (R_m), and photorespiration (R_p) are incorporated such that

$$Q_{\max} = [(P_{g1} + R_{m1} + R_{p1}) - (P_{g2} + R_{m2} + R_{p2})] / (PAR_1 - PAR_2), \quad (6)$$

where PAR_1 represents incident PAR as it approaches 0 and PAR_2 refers to the case when PAR is 0. Because the cuvette temperature was constant, we assume that $R_{m1} = R_{m2}$.

Because our method for determining quantum efficiency in the field illuminated leaf surfaces predominantly from only the upper side, the Q_{\max} values should be about half those determined on leaves receiving illumination from all sides within an integrating sphere (Leverenz & Öquist 1987; Ögren & Evans 1993).

Chlorophyll analyses were performed on deciduous leaves collected in August 1991 when leaves were fully green and in September 1991 when autumn colour was first noted using N, N-Di-methylformamide extraction (Moran & Porath 1980; Moran 1982; Inskeep & Bloom 1985). Leaf mass per unit area (LMA) was also determined to allow expression of results in mg chlorophyll per gram of tissue and mg chlorophyll per m^2 of leaf area. For red oak and red maple, 10 leaves were sampled and analysed from the upper and lower canopy strata. For other species, five leaves were collected from each stratum for analysis.

Quantum-use efficiency model

The quantum-use efficiency model assumes that photosynthetically active radiation (PAR) absorbed by the vegetation is converted into photosynthate based on the quantum efficiency of all leaves (Q_{\max} , g carbon fixed per mol photon). The maximum quantum efficiency (Q_{\max}) for the canopy was determined from photosynthesis measurements on upper canopy foliage of key species near the tower, weighted by the fraction of the total basal area that each species represented within the 50×50 m vegetation plot. We constrained the estimates of photosynthesis in this study to take into account partial or complete closure of stomata attributed to environmental factors, notably below-freezing conditions and extremes in vapour pressure deficits (VPD) (Law & Waring 1994a). The model predicts

gross ecosystem production (GEP) over a given time integral:

$$GEP = \sum (PAR * f_{IPAR}) Q_c, \quad (7)$$

where PAR is incident photosynthetically active radiation and f_{IPAR} is the fraction of incident PAR intercepted by vegetation. Q_c is the constrained quantum-use efficiency derived from multiplying Q_{\max} by values ranging from 0 (complete constraint on photosynthesis) to 1.0 (no environmental constraints), a convention which follows earlier work in Oregon on a variety of tree- and shrub-dominated landscapes where drought was an additional constraint on photosynthesis (Law & Waring 1994a; Runyon *et al.* 1994).

The constrained quantum-use efficiency model was driven with hourly meteorological data from the tower in Harvard Forest and parameterized separately for conifers and hardwoods, although the same Q_{\max} was applied to conifers for lack of other data. For the deciduous hardwoods, we specified the timing of leaf-off and assumed that no PAR was intercepted during that period. Phenological data from Harvard Forest indicated that 10–25% leaf-off occurred on 21 October 1991 and on 23 October 1992, and bud break occurred approximately on 6 May 1991 and on 13 May 1992. From the onset of deciduous leaf colour in autumn to the onset of leaf fall, we incrementally decreased Q_c from a maximum to zero to account for progressive reductions in chlorophyll during this transition period.

When temperatures were less than or equal to $-2^\circ C$, we assumed no light was utilized for photosynthesis for 24 h so that $Q_c = 0$. Each additional hour below this limit reduced Q_c to zero for another hour. The fractional reduction in Q_c caused by high VPD was applied hourly. We assumed no reduction for VPD less than 1.5 kPa and a linear reduction in the scalar between 1 and 0 for the fractional constraint between 1.5 and 2.5 kPa (Runyon *et al.* 1994; Law & Waring 1994a). The Q_c was determined hourly with a statistical programming package (SAS Institute, Inc., Raleigh, NC, USA) that incorporated meteorological data and the physiological constraints (Law & Waring 1994a).

Mean monthly f_{IPAR} , calculated from mean daily f_{IPAR} between 1000 and 1400 h, was combined with incident PAR to estimate intercepted PAR ($IPAR = f_{IPAR} * PAR$). Because the forest was a mixture of hardwoods and conifers, we determined the fraction of total f_{IPAR} for both components from the classification of cover fractions in video images obtained with the aircraft from the 1000×1000 m area around the tower (see next section for details).

Finally, GEP was calculated from Eqn 7 and summed monthly. These constrained quantum-use efficiency estimates of monthly GEP were regressed against those derived from eddy flux data. We also ran the quantum-use efficiency model with VPD constraints from eddy flux measurements made at Harvard Forest and compared the resulting monthly estimates of gross ecosystem production with the VPD response described earlier.

Remotely sensed measurements

From a Quicksilver Model GT-500 ultralight aircraft we collected remotely sensed data from altitudes of 300–400 and 1000 m and at an air speed of 55 km h⁻¹ over a 1000 × 1000 m area centred around the eddy flux tower. Flights were made between 0800 and 1200 on October 10 and April 10 1991, and on May 19 and July 6 1992. Video images were acquired continuously with a Sony Model TR5 8mm camera (230 000 images on a 2 h tape). Selected images were transferred to computer with a Matrox graphics board, and analysed with Resource Imaging Graphics System software (version 3.24, 1989; Decision Images, Inc., Princeton, NJ, USA). The spatial coverage of video images corresponds to a square with sides approximately equal to the altitude. Spatial resolution from an altitude of 1000 m altitude was 4 m². In April, when hardwoods were leafless, a supervised classification was performed on a total of 10 reference sites where patches of hardwoods and conifers were clearly evident. Image analyses to separate these two types were made over an increasing area (125 m × 125 m, 250 m × 250 m, 500 m × 500 m and 1000 m × 1000 m) centred on the eddy flux tower. Analyses were repeated three times to obtain standard errors of estimates.

Spectral reflectance measurements were collected at lower altitudes between 300 and 400 m to resolve differences between areas with conifer and hardwood cover. A Spectron Engineering SE-590 spectroradiometer (Denver, CO) was interfaced with a data logger. The SE-590 provides continuous spectra between 380 and 1100 nm at nominal 10 nm spectral resolution. In natural sunlight, instrument sensitivity is limited below 400 nm and above 900 nm (Goward, Huemmrich & Waring 1994b). We therefore limited the processing of data to the 400–900 nm range for all analysis reported in this paper. Equipped with a 1° lens, the circular resolution (R) in m² was determined from the formula:

$$R = \pi (\tan(\theta/2) h)^2, \quad (8)$$

where θ is the view angle in degrees and h is the altitude in m. At 300 m, the spatial resolution within a circular area was 21.5 m² with a diameter of 5.2 m. With a flight speed of 55 km h⁻¹ and an instrument scan time of 1 s, a rectangular ground area of 5.2 m × 15.3 m was captured. During all but the last sampling period we did not have a global positioning system (GPS) on board. This made it necessary to cross-link time codes on the video and spectroradiometer data to identify areas sampled.

Spectroradiometer data were edited to extract average reflectance values in the red (655–665 nm) and near-infrared (785–795 nm) acquired over specific types of cover identified from the time-linked video images. Software developed by Moon Kim (Goddard Space Flight Center, MD) was utilized in processing the reflectance data. The normalized difference vegetation index was calculated separately for areas dominated by conifer and by hardwood cover. Beneath these two distinct types of canopy, the fraction of intercepted light (f_{IPAR}) was mea-

sured under clear sky conditions in mid-afternoon following morning flights on three out of four dates; when deciduous trees were leafless in April, when they had begun leaf expansion in May, and when leaves were fully developed in July. No f_{IPAR} data were gathered in October when leaves were in full autumn colour.

To compare remotely sensed estimates of canopy leaf area and f_{IPAR} , separate estimates of f_{IPAR} for hardwoods and conifers were obtained with a single quantum sensor (Li-Cor, Lincoln, NE, USA) under clear sky conditions over an area of 0.5 ha. Seasonally, sample sizes ranged from 410 to 765 under the deciduous canopy and from 114 to 237 under the more uniform conifers. Light measurements were not made in October when canopy leaf area was still high but chlorophyll pigments had decreased. For reference, incident PAR was measured in the open before and after completion of measurements along the transects. The fraction of transmitted PAR was determined after log transformation to normalize for direct light penetration through canopy gaps (Lang & Yueqin 1986). The mean transformed value was back-transformed and subtracted from 1 to provide the mean fraction of intercepted PAR (f_{IPAR}), which was regressed against respective NDVI values.

RESULTS

Analysis of video images showed that, within the 125 × 125 m area centred on the eddy flux tower, conifers represented only about 7% of the cover (6.8% ± 0.7% SE). In contrast, a more representative sample for increasing larger areas centered on the tower indicated that conifers make up about 25% of the cover (250 × 250 m = 26.7% ± 1.2% SE; 500 × 500 m = 27.3% ± 0.2% SE; 1000 × 1000 m = 25.4 ± 0.2% SE).

The seasonal variation in f_{IPAR} determined from a pair of stationary quantum sensors appeared similar for both 1991 and 1992 (Fig. 1). Higher values of f_{IPAR} recorded in January than in April reflect differences in midday solar zenith angle, with more light interception by tree boles in January. The full canopy intercepted >80% of incident PAR from May to September. The measured light intercepted during the middle of the growing season was equivalent to that expected for a hardwood forest with a LAI of 3.2, applying the Beer-Lambert Law with an assumed extinction coefficient of 0.5. The values were similar to estimates of LAI made with a LiCor 2000 Plant Canopy Analyzer. The Plant Canopy Analyzer samples a hemispherical area, and may include the contribution of some scattered conifers in the estimates of projected LAI. Litter traps provided a range of LAI estimates between 2.7 and 4.1 for hardwoods.

The NDVI values for areas with pure hardwoods decreased from a maximum of 0.85 on 6 July 1992 to 0.61 on 10 October 1991 before a major decrease in f_{IPAR} was recorded near the tower (Table 1 & Fig. 1). The general relationship between mean NDVI measured separately over hardwoods and conifers and mean f_{IPAR} measured

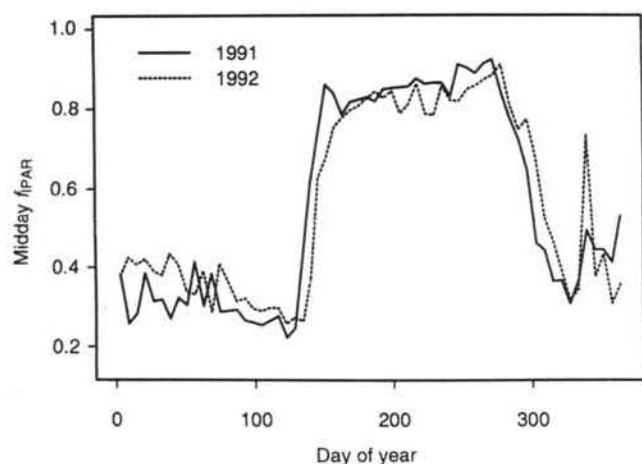


Figure 1. Midday fraction of photosynthetically active radiation intercepted (f_{IPAR}) by the predominately deciduous hardwood canopy near the eddy flux tower show similar patterns for 1991 and 1992, with full leaf display occurring between June and October.

Table 1. Seasonal variation in the fraction of photosynthetically active radiation intercepted (f_{IPAR}) by a canopy of deciduous hardwoods and evergreen conifers is compared with the normalized difference vegetation index (NDVI) determined from measurements made at an altitude of 300 to 400 m with an airborne spectroradiometer. Standard errors (SE) are provided. Sample sizes varied as noted *

Date	Type	f_{IPAR}	SE	NDVI	SE
April	hardwoods	0.504	0.024	0.430	0.011
April	conifers	0.918	0.081	0.840	0.009
May	hardwoods	0.495	0.026	0.590	0.029
May	conifers	0.913	0.081	0.850	0.006
July	hardwoods	0.845	0.033	0.880	0.002
July	conifers	0.933	0.028	0.870	0.003
October	hardwoods	–	–	0.610	0.020
October	conifers	–	–	0.860	0.005

*NDVI sample size = 20–25 for hardwoods and 3–5 for conifers. f_{IPAR} sample size = 410–765 for hardwoods and 114–237 for conifers.

beneath the two types of vegetation is presented in Fig. 2. We emphasize that the regression equation for Fig. 2 was developed for green foliage only and is not appropriate for application during leaf senescence because of the influence of chlorophyll on red reflectance. These restricted clear-weather measurements were not appropriate for comparison with daily mean values of transmitted PAR acquired from sensors near the tower.

The maximum quantum efficiency determined in mid-summer varied nearly 2-fold, from a low value of 0.026 mol C mol⁻¹ photon for *Acer rubrum* to a high of 0.047 mol C mol⁻¹ photon for *Betula alleghaniensis* (Table 2). When weighted by the representative basal area, which was 50% *Quercus rubra* and 30% for *Acer rubrum*, the average quantum efficiency at mid-summer was 0.0298

mol C mol⁻¹ photon or 0.36 g C mol⁻¹ photon (Q_{max}). We observed on 10 October 1991 that the NDVI values acquired from the ultralight aircraft would suggest that a fully green canopy had been reduced in leaf area since July by ~ 50% (from Fig. 2: NDVI = 0.61 is equivalent to an f_{IPAR} value of 0.63, which corresponds to an LAI ~ 2.0).

To account for seasonal differences in incident solar radiation, we calculated the ratio of the reflectance values recorded in the red (655–665 nm) and near-infrared (785–795 nm) bands against the total reflectance summed for all bands (400–900 nm). This normalizing procedure showed that reflectance in the red band increased from 3 to 6% between July and October, indicating a comparable reduction in chlorophyll absorption. Over the same period, near-infrared reflectance decreased by less than 30%, from 35 to 25.5% (R. W. McCreight, unpublished results). Phenological observations confirmed that only 10–25% of the leaves had fallen by 3 October 1991. The video image acquired on 10 October also confirmed that a dense canopy of hardwoods leaves was still present but in nearly full autumn colour (Fig. 3). We therefore interpreted the decrease in the hardwood NDVI in October (Table 1) to reflect mainly a reduction in chlorophyll absorption, which was confirmed by mid-September measurements that were nearly 50% below those measured in mid-August (Table 3).

We had hoped to identify species composition from video images acquired in October when hardwoods were in full colour, but were unsuccessful because colour differences varied with the precise stage in leaf senescence. An

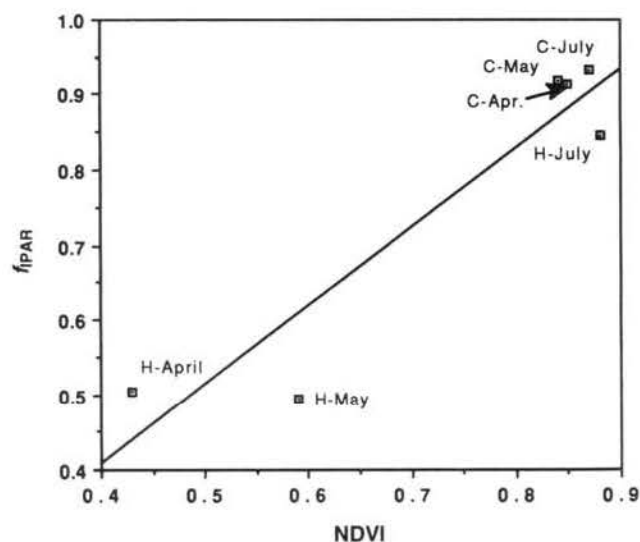


Figure 2. The normalized difference vegetation index (NDVI) determined over areas dominated by conifers (C) and deciduous hardwoods (H) indicates that essentially all seasonal variation is attributed to the hardwood component. $y = -0.01 + 1.050x$; $R^2 = 0.88$. October estimates of NDVI of 0.61 for areas with pure hardwoods correspond to an equivalent fraction of PAR interception (f_{IPAR}) of 0.63. The actual f_{IPAR} value, however, was still > 0.8 under the predominantly hardwood canopy near the tower (Fig. 1), indicating that NDVI integrates chlorophyll content as well as leaf area index (Table 3).

Table 2. Maximum quantum efficiency (Q_{\max} in mol C mol⁻¹ photon, and in g C mol⁻¹ photon) measured on five sets of individual leaves from the tops of canopies, and the fraction of total site basal area (BA)

Species	BA fraction	Q_{\max}	
		(mol C mol ⁻¹ photon)	(g C mol ⁻¹ photon)
<i>Quercus rubra</i>	0.50	0.0297	0.3564
<i>Acer rubrum</i>	0.30	0.0255	0.3060
<i>Betula papyrifera</i>	0.05	0.0394	0.4728
<i>Betula alleghaniensis</i>	0.05	0.0472	0.5664
Species-weighted mean		0.0298	0.3576

alternative means of assessing changes in the maximum quantum efficiency of the entire canopy with remote sensing was available through use of the recently established near-linear relations that exist between red reflectance (and NDVI) and chlorophyll concentrations in upper canopy leaves and between chlorophyll concentrations and photosynthetic capacity. These relationships have been confirmed for a variety of hardwood and conifer species with various spectral reflectance indices (Yoder & Waring 1994; Curran 1995; Gamon *et al.* 1995).

To confirm the first relation we compared the average chlorophyll concentrations measured on upper canopy leaves collected from the four species of hardwoods in August (Table 3) with their corresponding values of maximum quantum efficiency (Table 2). The correlation between chlorophyll concentration and Q_{\max} for upper

canopy leaves was linear with an R^2 of 0.99 (Fig. 4). These results suggest that seasonal estimates of NDVI or related reflectance indices may provide an integrated estimate of Q_{\max} for forests of mixed composition.

The constrained modelled quantum efficiency (Q_c) for conifers shown in Fig. 5, remained above 0.3 g C mol⁻¹ photon from April to October in both 1991 and 1992. The VPD proved to be only a minor constraint, reducing monthly net photosynthesis by a maximum of 8% in May 1991 and 6% in June 1992. Freezing temperatures reached a maximum constraint of 82% for conifers in January 1991 and 86% in February 1992. The combined climatic constraints resulted in estimates of Q_c for conifers which ranged from 0.07 g C mol⁻¹ photon in January to a maximum of 0.36 g C mol⁻¹ photon in September 1991, and from 0.05 g C mol⁻¹ photon in February to 0.36 g C mol⁻¹ photon in September 1992 (Fig. 5). The derived Q_c values were the same for hardwoods when green leaves were on the trees as for conifers, because the same quantitative environmental constraints were applied.

The quantum-use efficiency model estimates of GEP by hardwoods and conifers within the 125 × 125 m area around the tower during 1991 ranged from 0.45 g m⁻² month⁻¹ in January to 351 g m⁻² month⁻¹ in June (Table 4). For 1992, the range was from 0.55 g m⁻² month⁻¹ in February to 304 g m⁻² month⁻¹ in July. The annual sums were 1467 g m⁻² in 1991 and 1305 g m⁻² in 1992. The hardwoods accounted for 1328 g m⁻² in 1991, and 1177 g m⁻² in 1992 (90% of total).

Comparison of monthly GEP calculated from the quantum-use efficiency model using the standard VPD constraints versus those calculated from the flux estimates of VPD constraints showed no significant difference between

Species	Strata	Chl (mg g ⁻¹)	SD (mg g ⁻¹)	SLA (mg cm ⁻²)	SD (mg cm ⁻²)	Chl (mg m ⁻²)
<i>August</i>						
red oak	lower	6.88	1.81	5.46	0.96	376
red oak	upper	4.37	0.84	8.22	0.87	360
red maple	lower	7.24	1.11	5.05	0.60	366
red maple	upper	3.52	0.66	9.76	1.06	343
white birch	lower	6.34	0.43	5.67	0.49	360
white birch	upper	4.65	0.24	8.65	0.84	402
yellow birch	lower	9.15	0.48	4.10	0.37	375
yellow birch	upper	4.57	0.55	9.83	1.21	449
August Average						379 ± 33
<i>September</i>						
red oak	lower	2.66	1.65	4.92	0.72	131
red oak	upper	1.70	0.64	8.96	0.79	152
red maple	lower	4.57	0.64	5.79	1.44	264
red maple	upper	2.45	0.56	8.72	1.37	214
white birch	lower	3.31	1.24	6.94	1.28	230
white birch	upper	2.03	0.50	8.76	0.85	178
yellow birch	lower	7.14	0.71	3.55	0.25	254
yellow birch	upper	2.73	1.13	5.61	0.53	153
September average						197 ± 50*

Table 3. Seasonal changes in chlorophyll concentrations and specific leaf area (SLA) with standard deviations (SD) determined on 5–10 leaves collected from the top and lower canopy in August and September 1991

* $P = 0.0002$



Figure 3. A photograph of autumn colouration at Harvard Forest taken from an ultralight aircraft flying at 300m above the canopy and tower installation. The picture was taken by R. W. McCreight with a Canon 35 mm camera set at 250th s with K200 slide film.

estimates. Monthly GEP estimates from the quantum-use efficiency model and from the flux residual approach were also similar throughout the year (Figure 6, Table 4). A linear regression of monthly GEP estimated using the two separate approaches showed a high correlation (Fig. 7; 1991 $R^2 = 0.97$; 1992 $R^2 = 0.99$). The slope was slightly, but significantly, different from unity in 1992 ($P = 0.01$), but not in 1991 ($P = 0.11$). The intercept was essentially zero in both years ($P = 0.52$ for both years).

When conifer cover was increased from 7% for the 125

$\times 125$ m area to 25% representative of larger areas up to 1000×1000 m, the model predicted a maximum monthly increase in photosynthesis during the months of April and October of 14 to 18 g C m^{-2} when hardwood trees were leafless (data not shown). At these times temperatures were still above freezing and PAR was well above the light compensation point for conifers (Fig. 1). Model estimates of annual GEP increased by only 4–5%, to $1525 \text{ g m}^{-2} \text{ year}^{-1}$ in 1991 and to $1369 \text{ g m}^{-2} \text{ year}^{-1}$ in 1992 by an increase in conifer cover from 7 to 25%.

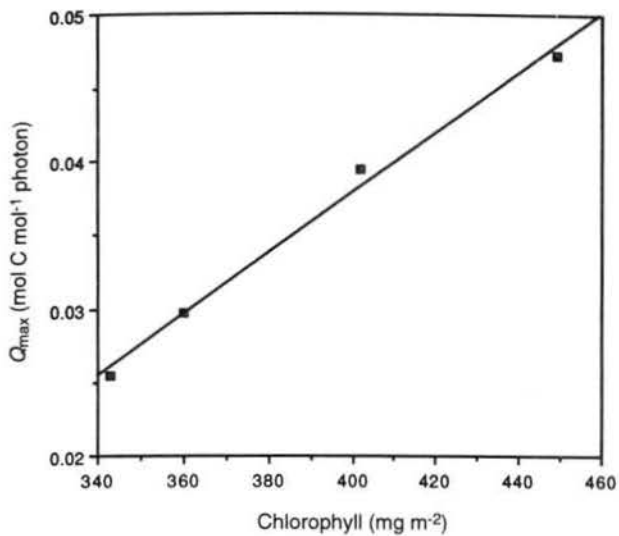


Figure 4. Mean values of chlorophyll concentrations from the upper canopy leaves of four hardwood species (Table 3) were linearly related to the maximum quantum efficiency (Q_{\max}) determined on the same leaves in August (Table 2). $y = -0.044 + 0.0002x$; $R^2 = 0.99$. Sample size varied from 5 to 10 leaves with the higher numbers collected from the dominant oaks and maples.

DISCUSSION

The quantum-use efficiency model requires an accurate estimate of the apparent maximum quantum efficiency derived from cuvette gas-exchange measurements in the upper, most active canopy strata. We were fortunate to have tower access and to sample on days with high humidity so that VPD had little effect on stomata and thus Q_{\max} . In more arid environments, cuvettes with environmental controls would be required to obtain maximum values of quantum efficiency. The weighting by species fraction of the total site basal area appears to be a reasonable approach

to estimating the average Q_{\max} . The oak and maple leaves collected in litter traps for both 1991 and 1992 represented 75–90% of the total leaf area collected whereas their basal area was 80% of the total (conifer basal area was ~10% but is not listed in Table 3).

In more open canopies, or canopies with lower quantum efficiencies, the assumption of linearity between light interception and photosynthetic activity may not be as valid as a curvilinear light-saturation model (McCree

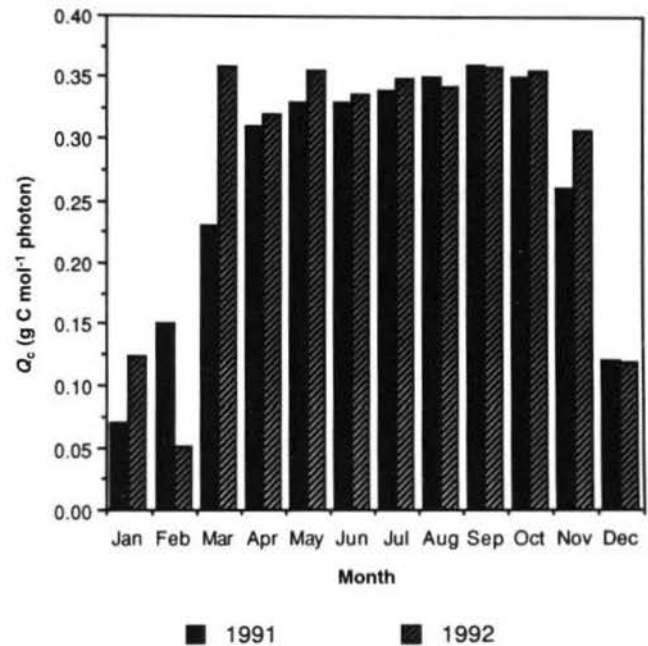


Figure 5. Combined climatic constraints of subfreezing temperatures and extremes in VPD resulted in estimates of quantum-use efficiency (Q_c) for conifers ranging from 0.07 g C mol⁻¹ photon in January to a maximum of 0.36 g C mol⁻¹ photon in September 1991, and from 0.05 g C mol⁻¹ photon in February to 0.36 g C mol⁻¹ photon in September 1992.

Month	1991			1992		
	Hardwoods	Total Site		Hardwoods	Total Site	
	Quantum	Quantum	Flux	Quantum	Quantum	Flux
Jan	0.00	0.45	23.17	0.00	1.01	-3.93
Feb	0.00	1.93	21.05	0.00	0.55	4.99
Mar	0.00	3.16	0.00	0.00	3.92	1.41
Apr	0.00	5.99	49.77	0.00	5.87	24.00
May	136.82	151.43	121.99	95.55	109.15	92.46
Jun	323.65	351.22	304.90	267.98	290.81	257.27
Jul	300.71	326.33	329.20	279.82	303.66	299.97
Aug	302.58	328.36	313.67	250.21	271.52	247.36
Sep	233.75	254.09	188.41	221.61	240.57	199.16
Oct	30.64	40.90	52.41	61.56	74.59	68.85
Nov	0.00	2.30	10.21	0.00	2.80	22.28
Dec	0.00	1.13	-15.94	0.00	0.84	4.08
Total	1328.15	1467.29	1398.84	1176.73	1305.29	1217.90

Table 4. Estimates of monthly gross photosynthesis (g m⁻² month⁻¹) from the quantum-use efficiency model (Quantum) and from eddy flux estimates (Flux) for 1991 and 1992. Model estimates assume conifer cover at 7%, hardwoods at 93%

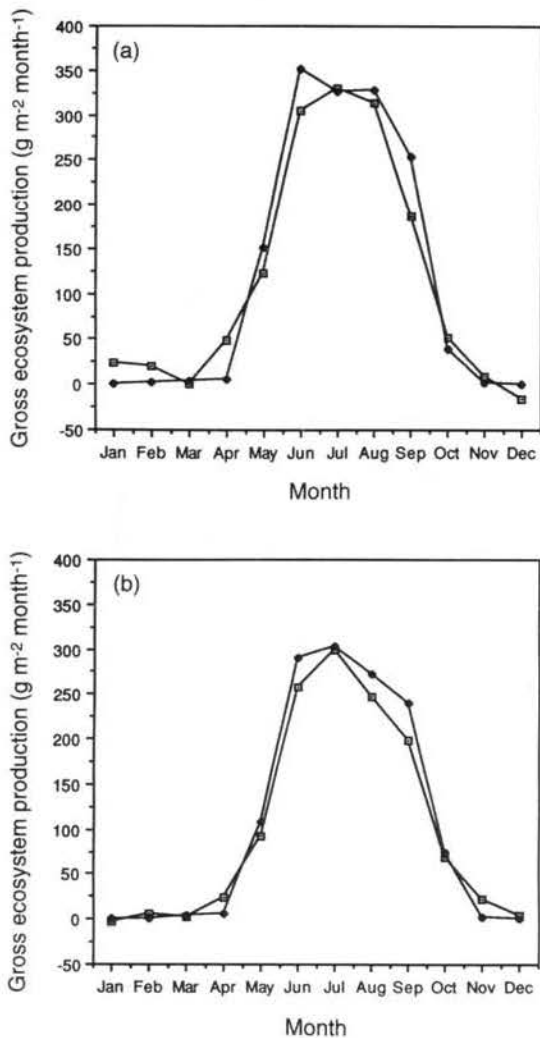


Figure 6. Monthly integrated estimates of gross ecosystem production (GEP) made with the constrained quantum-use efficiency model agreed well with those derived from continuous flux measurements of CO_2 in both 1991 (a) and 1992 (b). —□—, flux estimate; —◆—, model estimate.

1984; Hollinger *et al.* 1994). With a monthly resolution, it seems appropriate to treat the canopy as a single unit, particularly when f_{IPAR} values are acquired continuously and include overcast and clear sky conditions. Other studies have demonstrated that in moderately dense deciduous hardwood canopies, near-linear relations exist between light conditions and leaf mass m^{-2} foliage, nitrogen content m^{-2} of foliage, and photosynthetic capacity (Ellsworth & Reich 1993). Similar reports have also been published for evergreen hardwoods (Hollinger 1989) and for conifers (Oren *et al.* 1986), suggesting that estimates of quantum efficiency may be similar for leaves throughout closed canopies (Wang & Polglase 1995).

We were concerned that high photosynthetic rates on one day might cause accumulations of starch that would lead to photosynthetic inhibition on proceeding days (Luxmoore 1991). From inspection of data, however, we found little indication that previous high rates of photosyn-

thesis in the preceding 1 to 24 h affected observed rates (M. L. Goulden, unpublished results).

In applying the quantum efficiency model, we assumed that common physiological thresholds apply to all species. We also ignored the possibility of delayed response to subfreezing or abnormally high temperatures (Leverenz & Öquist 1987; Bassow, McConnaughay & Bazzaz 1994). We recognize that species differ in the rates in which their stomata respond to light fluctuations, VPD and other environmental factors (Schulze *et al.* 1994). Because hourly data are integrated over monthly periods, however, errors in determining physiological thresholds are less critical than for models that predict in shorter time steps.

In this study, the major environmental constraint on canopy photosynthesis was IPAR. Subfreezing tempera-

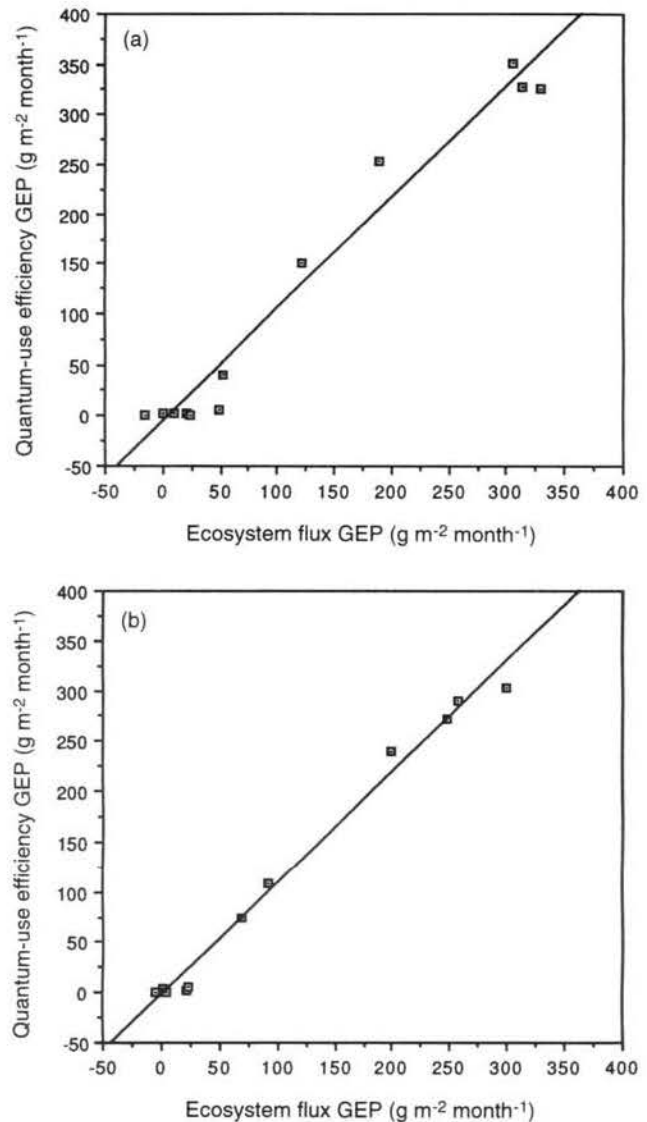


Figure 7. The regression of monthly integrated estimates of gross ecosystem production (GEP) made by the constrained quantum-use efficiency model was linearly related to monthly integrated values obtained from ecosystem flux measurements at the tower in both (a) 1991 ($y = -7.365 + 1.112x$; $R^2 = 0.97$) and (b) 1992 ($y = -3.775 + 1.109x$; $R^2 = 0.99$).

tures had a significant effect only on the conifers during mid-winter at the time deciduous trees were leafless. Vapour pressure deficits were not extreme during the summer and therefore had little effect on Q_c . VPD and sub-freezing temperatures restrict photosynthesis by 50–75% in shrub and evergreen forest vegetation in temperate regions such as the Pacific Northwest of the USA (Runyon *et al.* 1994; Law & Waring 1994a) and to a somewhat lesser extent on the South Island of New Zealand (Hollinger *et al.* 1994).

Good agreement between the constrained quantum-use efficiency estimates of GEP and those determined from two years of eddy flux measurements further supports the value of integrating at monthly time steps. It is not reasonable to expect model predictions to agree well with hourly or daily measurements of photosynthesis because varying quantities of direct and diffuse radiation influence photosynthetic efficiency differently. Diffuse light casts less shadow and therefore penetrates more efficiently through canopies. As a result, photosynthetic rates may not decrease as much as expected (Sheehy & Chapas 1976; Hollinger *et al.* 1994; Fan *et al.* 1995). Our approach may have partly solved this problem by obtaining f_{IPAR} values under a range of cloud conditions each month and by integrating model estimates of photosynthesis at monthly intervals.

We recognized that flux measurements taken from a single stationary tower may not represent gas exchange from a large forest (Hollinger *et al.* 1994). When conifers are clumped in their distribution, the wind direction may have a major influence on their contribution to area-wide fluxes. Similarly, restricted area sampling of f_{IPAR} measurements can bias estimates of photosynthesis if the sampling is not representative of the larger area. Both of these problems can be solved in part by measuring fluxes and remotely sensing canopy properties from aircraft (Dejardins *et al.* 1982; Spanner *et al.* 1994).

Scaling of the quantum-use efficiency model to larger areas may be accomplished through satellite or airborne estimates of f_{IPAR} and Q_{max} . Satellite estimates of f_{IPAR} require atmospheric correction, in particular for visible wavelengths. Low-altitude airborne sensors provide an advantage by acquiring reflectance data with little atmosphere between the ground and the sensor. Data acquired from aircraft can also validate atmospheric corrections modelled for satellite data (Goward *et al.* 1994a). In regions where snow cover is likely, NDVI estimates would be misrepresentative of canopy properties. We recommend obtaining minimum estimates of f_{IPAR} for the year by concentrating observations on clear days in the spring or autumn when deciduous trees are not in leaf to minimize effects of snow cover. Where evergreens dominate, seasonal variation in leaf area is often less than 30% (Spanner *et al.* 1994).

The potential exists for scaling the quantum-use efficiency model to biomes and the globe, as suggested by Running & Hunt (1993). A physiological model (BIOME-BGC) is available to estimate Q_c from climatic data and

certain biome-specific assumptions about nitrogen, carbon, and water movement through the system (Running *et al.* 1994). Meteorological data are also necessary as driving variables in this approach, and have been successfully estimated across mountainous topography where temporary weather stations were installed for validation (Glassy & Running 1994). An alternative would be to apply the simplified constraints of freezing temperature, drought, and high VPD to Q_{max} , using remote sensing to estimate the meteorological variables as well as f_{IPAR} and incident PAR (Goward *et al.* 1994a; Prince & Goward 1995).

We recommend that monthly resolution models of net photosynthesis and other ecosystem properties should be tested where continuous flux measurements are being made throughout the year. Harvard Forest is one of the first sites to attempt these long-term measurements (Wofsy *et al.* 1993). To scale predictions to larger areas, remote sensing of red and near-infrared reflectance, coupled with video analysis to resolve variation in deciduous and evergreen cover, showed promise as a viable approach at Harvard Forest.

ACKNOWLEDGMENTS

We thank John O'Keefe for providing hardwood phenological information at Harvard Forest, Gody Spycher for his assistance in preparing the meteorological data files for model analyses, and Tony Olsen for statistical advice. To support this work Harvard University received grants from the National Science Foundation (BSR-89-19300), the National Aeronautics and Space Administration (NAGW-3082), and the Department of Energy (Northeast Regional Center of the National Institute for Global Environmental Change) and from Harvard University (Harvard Forest and Division of Applied Science). At Oregon State University the work was supported by grants from the Northeast Regional Center of the National Institute for Global Environmental Change, Harvard University and from the National Aeronautics and Space Administration (NAGW-3642) to support the Program for Airborne Environmental Analysis.

REFERENCES

- Asrar G., Fuchs M., Kanemasu E.T. & Hatfield J.L. (1984) Estimating absorbed photosynthetic radiation and leaf area index from spectral reflectance in wheat. *Agronomy Journal* **76**, 300–306.
- Baker D.N., Hesketh J.D. & Duncan W.G. (1972) Simulation of growth and yield in cotton: I. Gross photosynthesis, respiration, and growth. *Crop Science* **12**, 431–435.
- Baldocchi D.D. & Meyers T.P. (1991) Trace gas exchange above the floor of a deciduous forest. I. Evaporation and CO₂ efflux. *Journal of Geophysical Research* **96**, 7271–7285.
- Bassow S.L., McConnaughay K.D.M. & Bazzaz F.A. (1994) The response of temperate tree seedlings grown in elevated CO₂ to extreme temperature events. *Ecological Applications* **4**, 593–603.

- Caldwell M.M., Meister H.-P., Tenhunen J.D. & Lange O.L. (1986) Canopy structure, light microclimate and leaf gas exchange of *Quercus coccifer* L. in a Portuguese macchia: measurements in different canopy layers and simulations with a canopy model. *Trees* **1**, 25–41.
- Charles-Edwards, D.A. (1982) *Physiological Determinants of Crop Growth*. Academic Press, Sydney, Australia.
- Curran, P.J. (1995) Exploring the relationship between reflectance red edge and chlorophyll concentration in slash pine leaves. *Tree Physiology* **15**, 203–206.
- Desjardins R.L., Brach E.J., Alvo P. & Schuepp P.H. (1982) Aircraft monitoring of surface carbon dioxide exchange. *Science* **216**, 733–735.
- Dye D.G. & Goward S.N. (1993) Photosynthetically active radiation absorbed by global land vegetation in August 1984. *International Journal of Remote Sensing* **14**, 3361–3364.
- Ellsworth D. & Reich P.B. (1993) Canopy structure and vertical patterns of photosynthesis and related leaf traits in a deciduous forest. *Oecologia* **96**, 169–178.
- Fan S.-M., Goulden M.L., Munger J.W., Daube B.C., Bakwin P.C., Wofsy S.C., Amthor J.S., Fitzjarrald D.R., Moore K.E. & Moore T.R. (1995) Environmental controls on the photosynthesis and respiration of a boreal lichen woodland: a growing season of whole-ecosystem exchange measurements by eddy correlation. *Oecologia* **102**, 443–452.
- Gamon, J.A., Field, C.B., Goulden, M.L., Griffin, K.L., Hartley, A.E., Joel, G., Peñuelas, J. & Valentini, R. (1995). Relationships between NDVI, canopy structure, and photosynthesis in three Californian vegetation types. *Ecological Applications* **5**, 28–41.
- Glassy J.M. & Running S.W. (1994) Validating diurnal climatology logic of the MT-CLIM model across a climatic gradient in Oregon. *Ecological Applications* **4**, 248–257.
- Goward S.N., Waring R.H., Dye D.G. & Yang J. (1994a) Ecological remote sensing at OTTER: Satellite macroscale observations. *Ecological Applications* **4**, 322–343.
- Goward S. N., Huemmrich, K. F. & Waring R. H. (1994b). Visible-near infrared spectral reflectance of landscape components in Western Oregon. *Remote Sensing of Environment* **47**, 190–203.
- Hollinger, D.Y. (1989). Canopy organization and foliage photosynthetic capacity in a broad-leaved evergreen montane forest. *Functional Ecology* **3**, 53–62.
- Hollinger D.Y., Kelliher F.M., Byers J.N., Hunt J.E., McSeverny T.M. & Weir P.L. (1994) Carbon dioxide exchange between an undisturbed old-growth temperate forest and the atmosphere. *Ecology* **75**, 134–150.
- Inskip W.P. & Bloom P.R. (1985) Extinction coefficients of chlorophyll a and b in N, N-Dimethylformamide and 80% acetone. *Plant Physiology* **77**, 483–485.
- Jarvis P.G. & Leverenz J.W. (1983) Productivity of temperate, deciduous, and evergreen forests. In *Encyclopedia of Plant Physiology*, Vol. 12B (eds O.L. Lange, P.S. Nobel, C.B. Osmond & H. Ziegler), pp. 233–280. Springer-Verlag, New York.
- Kumar M. & Monteith J.L. (1982) Remote sensing of plant growth. In *Plants and the Daylight Spectrum* (ed. H. Smith), pp. 133–144. Academic Press, London.
- Landsberg J.J. (1986) *Physiological Ecology of Forest Production*. Academic Press, London.
- Lang A.R.G. & Yuequn X. (1986) Estimation of leaf area index from transmission of direct sunlight in discontinuous canopies. *Agricultural & Forest Meteorology* **37**, 229–243.
- Law B.E. & Waring R.H. (1994a) Combining remote sensing and climatic data to estimate net primary production across Oregon. *Ecological Applications* **4**, 717–728.
- Law B.E. & Waring R.H. (1994b) Applying spectral indices to estimate leaf area index and radiation intercepted by understory vegetation. *Ecological Applications* **4**, 272–279.
- Lee, X. & Black, T.A. (1994) Relating eddy correlation sensible heat flux to horizontal sensor separation in unstable atmospheric surface layer. *Journal of Geophysical Research* **99**, 18545–18553.
- Leuning R. & King K.M. (1992) Comparison of eddy-covariance measurements of CO₂ fluxes by open- and closed-path CO₂ analyzers. *Boundary Layer Meteorology* **59**, 297–311.
- Leverenz L.W. & Öquist G. (1987) Quantum yields of photosynthesis at temperatures between –2°C and 35°C in a cold-tolerant C-3 plant (*Pinus sylvestris*) during the course of one year. *Plant, Cell and Environment* **10**, 287–295.
- Luxmoore R.J. (1991) A source-sink framework for coupling water, carbon, and nutrient dynamics of vegetation. *Tree Physiology* **9**, 267–280.
- McCree K.J. (1984) Daily photosynthesis totals calculated from solar radiation histograms. *Agricultural & Forest Meteorology* **33**, 239–248.
- McMillen R.T. (1988) An eddy correlation technique with extended applicability to non-simple terrain. *Boundary Layer Meteorology* **43**, 321–245.
- Melillo J.M., McGuire A.D., Kicklighter D.W., Moore B.I., Vorosmarty C.J. & Schloss A.L. (1993). Global climate change and terrestrial net primary production. *Nature* **363**, 234–240.
- Moran R. (1982) Formulae for determination of chlorophyllous pigments extracted with N, N-Dimethylformamide. *Plant Physiology* **69**, 1376–1381.
- Moran R. & Porath D. (1980) Chlorophyll determination in intact tissues using N, N-Dimethylformamide. *Plant Physiology* **65**, 478–479.
- Nemani R., Pierce L. & Running S. (1993) Developing satellite-derived estimates of surface moisture status. *Journal of Applied Meteorology* **32**, 548–557.
- Ögren E., & Evans J.R. (1993) Photosynthetic light-response curves: I. The influence of CO₂ partial pressure and leaf inversion. *Planta* **189**, 182–190.
- Oren R., Schulze E.-D., Matussek R. & Zimmermann R. (1986) Estimating photosynthetic rate and annual carbon gain in conifers from specific leaf weight and leaf biomass. *Oecologia* **70**, 187–193.
- Peterjohn W.T., Melillo, J.M., Steudler P.A., Newkirk K.M., Bowles F.P. & Aber J.D. (1994). Responses of trace gas fluxes and N availability to experimentally elevated soil temperatures. *Ecological Applications* **4**, 617–625.
- Potter C.S., Randerson J.T., Field C.B., Matson, P.A.S., Vitousek P.M., Mooney H.A. & Klooster S.A. (1994) Terrestrial ecosystem production: a process model based on global satellite and surface data. *Global Biogeochemical Cycles* **7**, 811–841.
- Prince S.D. & Goward S.N. (1995) Global primary production: a remote sensing approach. *Global Ecology and Biogeography Letters* (in press).
- Running S.W. & Hunt R. Jr (1993) Generalization of a forest ecosystem process model for other biomes, BIOME-BGC, and application for global-scale models. In *Scaling Physiological Processes: Leaf to Globe* (eds J.R. Ehleringer & C.B. Field), pp. 141–158. Academic Press, Inc., San Diego, CA.
- Running S.W., Nemani R.R., Peterson D.L., Band L.E., Potts D.F., Pierce L.L. & Spanner M.A. (1989) Mapping regional forest evapotranspiration and photosynthesis by coupling satellite data with ecosystem simulation. *Ecology* **70**, 1090–1101.
- Running S.W., Justice C.O., Salomonson V., Hall D., Barker J., Kaufmann Y.J., Strahler A.H., Huete A.R., Muller J.-P., Vanderbilt V., Wan Z.M., Teillet P. & Carneggie D. (1994) Terrestrial remote sensing science and algorithms planned for EOS/MODIS. *International Journal of Remote Sensing* **15**, 3587–3620.
- Runyon J., Waring R.H., Goward S.N. & Welles J.M. (1994)

- Environmental limits on net primary production and quantum-use efficiency across the Oregon Transect. *Ecological Applications* **4**, 226–237.
- Schulze E.-D., Kelliher F.M., Körner C., Lloyd J., & Leuning R. (1994). Relationships between maximum stomatal conductances, ecosystem surface conductance, carbon assimilation rate and plant nitrogen nutrition: A global ecology scaling exercise. *Annual Review of Ecology and Systematics* **25**, 625–660.
- Sellers P.J., Berry J.A., Collatz G.J., Field C.B. & Hall F.G. (1992) Canopy reflectance, photosynthesis, and transpiration. III. A reanalysis using improved leaf models and a new canopy integration scheme. *Remote Sensing of Environment* **42**, 187–216.
- Sheehy J.E. & Chapas L.C. (1976) The measurement and distribution of irradiance in clear and overcast conditions in four temperate forage grass canopies. *Journal of Applied Ecology* **13**, 831–840.
- Spanner M., Johnson L., Miller J., McCreight R., Freemantle J., Runyon J. & Gong P. (1994) Remote sensing of seasonal leaf area index across the Oregon transect. *Ecological Applications* **4**, 258–271.
- Tans P.P., Fung I.Y. & Takahashi T. (1990). Observational constraints on the global atmospheric CO₂ budget. *Science* **247**, 1431–1438.
- Verma S.B., Sellers P.J., Walthall C.L., Hall F. G., Kim J. & Goetz S. J. (1993) Photosynthesis and stomatal conductance related to reflectance on the canopy scale. *Remote Sensing of Environment* **44**, 103–116.
- Wang Y.P. & Polglase P.J. (1995) The carbon balance in the tundra, boreal and humid tropical forests during climate change - scaling up from leaf physiology and soil carbon dynamics. *Plant, Cell and Environment* **18**, 1226–1244 (this issue).
- Wang Y.P., McMurtrie R.E. & Landsberg J.J. (1992) Modelling canopy photosynthetic productivity. In *Crop Photosynthesis: Spatial and Temporal Determinants* (eds N.R. Baker & H. Thomas), pp. 43–67. Elsevier Science Publishers, Amsterdam, The Netherlands.
- Waring R.H., Runyon J., Goward S.N., McCreight R., Yoder B. & Ryan M.G. (1993) Developing remote sensing techniques to estimate photosynthesis and annual forest growth across a steep climatic gradient in western Oregon, U.S.A. *Studia Forestalia Suecica* **191**, 33–42.
- Welles J.M. & Norman R. (1991) Instrument for indirect measurement of canopy architecture. *Agronomy Journal* **83**, 818–825.
- Wofsy S.C., Goulden M.L., Munger J.W., Fan S.-M., Bakwin P.S., Daube B.C., Bassow S.L. & Bazzaz F.A. (1993) Net exchange of CO₂ in a mid-latitude forest. *Science* **260**, 1314–1317.
- Yoder B.J. & Waring R.H. (1994) The normalized difference vegetation index of small Douglas-fir canopies with varying chlorophyll concentrations. *Remote Sensing of Environment* **49**, 81–91.